In response to the comments we received from the editor and from the reviewers we have re-written most of the manuscript including:

1. Adding the dimensional vorticity equation

2. Re-writing the entire text with ε as the non-dimensional friction coefficient instead of α

3. Producing new versions of the four figures including new simulations with fixed values of the new friction parameter

4. Adding a detailed description in the Discussion regarding the ramifications of our results to the Sverdrup solution in the interior of the basin (that drives the poleward directed transport in the WBC)

A point-by-point response to the particular comments, including pointers to the text where these changes were implemented follows. A marked up manuscript version in which the differences between the new and previous versions are clearly marked is uploaded as a separated file.

Subject: Authors' response to RC1 and corresponding changes to the MS.
We thank the referee for helping us improve the quality of our paper. In the following we address the minor comments raised in the review.

While I agree that non-dimensional equations are useful, it is unclear what the new physical findings of this study are. Is there a change in how the vorticity balances in the western boundary layer? The authors need to clarify that the parameter dependence of the WBC solution is not just a result of the mathematical formulation that the authors have chosen.

Response: While the role of damping (α or ϵ in our formulation) in the westward intensification has been previously discussed extensively in the literature, the dependence of the WBC's transport on the domain aspect ratio has not been studied (save for its mention in Bye and Veronis, 1979). The novel finding of our study is the first quantification of the dependence of the WBC's transport on the domain aspect ratio. This finding enables, in turn, its application to the five known WBCs.

Clearly, the vorticity balance in the boundary layer is unaffected by our scaling but in the interior of the basin our formulation and scaling shows that the term of the Laplacian proportional to $\partial^2\psi/\partial y^2$ can be neglected only for $\delta \geq 1$ (see our detailed response to the next comment). Our concise formulation underscores features that exist in the dimensional formulation (as in our numerical simulations) but are hard to see when dealing with five model parameters.

(1) I would like the authors to discuss the sensitivity of the results to the choice of the boundary current width. In terms of mass balance, the WBC simply returns the Sverdrup interior so if the Sverdrup interior is kept constant, the transport of the WBC will not change. The meridional velocity at the western boundary also varies differently in the zonal direction for S48 and M50: for S48, it decays exponentially with epsilon while for M50, a maximum occurs near epsilon. The way the transports are estimated (Equations 4 and 8) does not seem to fully take these differences into account.

Response: It is indeed correct that the WBC's transport is equal in magnitude to the Sverdrup transport in the basin's interior. However, the Sverdrup transport itself is dependent on the basin's aspect ratio. The correction to the Sverdrup transport in bounded domains was developed in Bye and Veronis (1979).

In terms of our scaling this correction can be derived by noting that since $\alpha = \epsilon/\delta^2$, equation (1) of the manuscript implies:

$$\left(\epsilon\frac{\partial^2}{\partial x^2} + \frac{\epsilon}{\delta^2}\frac{\partial^2}{\partial y^2}\right)\psi + \frac{\partial \psi}{\partial x} = \sin(\pi y)$$

where $\epsilon = (r/\beta L_x)$ is a proxy of damping and the non-dimensional width of the WBC. Under the assumption of small damping i.e. $\epsilon \ll 1$, the term $\frac{\epsilon}{\delta^2}\frac{\partial^2\psi}{\partial y^2}$, cannot be neglected in the interior solution when $\delta^2 \sim O(\epsilon)$ i.e. the Sverdrup balance becomes a function of δ in this case. As was rightly pointed out by the referee, the WBC 'simply returns' this δ-dependent Sverdrup transport.

We employed the simple scaling to obtain our ad-hoc definition of the boundary layer width [i.e. $\epsilon = r/(\beta L_x)$ for Stommel's model and $\epsilon = [\mu/(\beta L_x^3)]^{(1/3)}$ for Munk's model] to make the paper more accessible to oceanographers that are inclined towards observations or numerical modeling. Equations (4) and (8) are of the form:

$$Tr = \frac{\delta}{\alpha\pi^2}[1 - O(\epsilon)] \qquad (4')$$

and

$$Tr = \delta[1 - O(\epsilon)] \qquad (8')$$

These expressions are valid for values of ϵ for which a WBC exists and they show that our results are not sensitive to the precise definition of the WBC's width. For instance, the width of the WBC can also be defined as the value of x for which the stream function reaches an extrema. By this definition, $\epsilon_S \sim 5\epsilon$ for Stommel's and $\epsilon_M \sim 2\epsilon$ for Munk's model, where ϵ is the current definition of the WBC's width in the two models. The respective transports in the two cases are given by:

$$Tr_S = \frac{\delta}{\alpha\pi^2}(1 - pe^{5A\epsilon} - qe^{5B\epsilon})$$

and

$$Tr_M = \delta\left(1 - e^{-1}\left[\cos(\sqrt{3}) + \frac{1-2\epsilon}{\sqrt{3}}\sin(\sqrt{3})\right]\right)$$

Here, we see that the two transports calculated by the new definition of WBC's width are also of the form (4') and (8'), which indicates that the results presented in this paper are independent of the precise definition of WBC's width. We thank the referee for this comment and we will further highlight the independence of our results to the choice of WBC's width in the revised manuscript.

Changes: Lines 121 - 126 in the revised version of the manuscript discuss how our results are independent of the definition of the WBC's width.

(2) The scaling of the stream function depends on delta $[\gamma\beta L_y^3 = \tau\pi/(\rho H_0\beta\delta)]$. Is the sensitivity of the WBC transport to δ a consequence of using such a scaling? As L_y changes, so do the magnitude of the wind stress curl and the scaling of the stream function. What is the benefit of using such scaling? To focus on the WBC, isn't it better to keep the wind stress curl constant and keep the Sverdrup interior the same?

Response: No, the sensitivity of the WBC's transport to δ is not a consequence of using our particular scaling. To appreciate this subtle dependence one should compare a square basin, where $\delta = 1$, with a "narrow and long channel-like" basin where $\delta \ll 1$. In a square basin, the classical approach of equating $\partial\psi/\partial x$ to $\sin(\pi y)$ works well since the North-South gradient of the zonal velocity (represented by $\partial^2\psi/\partial y^2$) is small and can be neglected from the interior solution. However, in a "channel-like" ocean this quantity is large and cannot be neglected from the balance of terms in the interior solution. Surely, an examination of the 3 vorticity terms in the interior ($\partial\psi/\partial x$, wind-stress and $\partial^2\psi/\partial y^2$) clarifies that the WBC in the "channel-like" ocean should be weaker compared to a square ocean.

As in all non-dimensional problems, the choice of scaling is not unique. We choose this scaling to stay consistent with the one proposed in Bye and Verionis, 1979. The results are independent of magnitude of wind-stress curl because the differential operators in the vorticity equations of Stommel and Munk are all linear.

We thank the reviewer for this comment and we include the aforementioned example in the revised manuscript to further elaborate the conceptual aspect of our paper. We will also re-write the paper with ϵ as the damping parameter (instead of α) in both Stommel and Munk models.

Changes: The entire paper was re-written with ϵ as the damping parameter (instead of α). Furthermore, lines 232 - 262 in the revised version of the manuscript highlight why the conceptual aspect of this paper is not a consequence of the scaling employed. This part of the discussion underscores the 'physical' meaning of the vorticity terms in the interior of the basin in both models and presents our results in a more intuitive framework.

(3) Figure 4 shows that the transport of the East Australian Current (EAC) is weaker than the other WBCs because of the small delta. But how was Ly determined for EAC? The meridional scale of this western boundary current appears to be different from the spatial scale of the winds. Zero wind stress curl does not exist around 22S (e.g. https://booksite.elsevier.com/DPO/chapterS10.html)

Response: The conflict between the geometry of the ocean basin and the overlying wind stress in the WBCs is independent of the model used for explaining the properties of the WBCs and hence does not affect our formulation and scaling. In appendix C of our paper we discuss in detail how the irregular shaped basin in the world ocean were approximated to obtain values of L_x and L_y. The error-bars along the ordinate provide a range between which δ can vary for different choices of L_y and L_x.

Changes: No changes were made per this minor comment because addressing the issue highlighted by the referee in this comment is beyond the scope of this study.

References:

Bye, J. A. T., and George Veronis. "A correction to the Sverdrup transport." Journal of Physical Oceanography 9.3 (1979): 649-651.

Subject: Authors' response to RC2 & RC3 and the corresponding changes to the MS.

We thank the referee for helping us improve the quality of our paper. However, the referee's (single) major comment is completely irrelevant to our analysis of Stommel's model. Furthermore, the recommendation to reject our manuscript completely ignores our (unchallenged) analysis of Munk's model.

While it was an enjoyable exercise to revisit the general solutions of these classical models, I'm afraid that I am unable to recommend the manuscript for publication as I believe the results are misleading, at least in the parts of parameter space of most relevance to the ocean (and it is debatable that these models are of any quantitative relevance beyond their substantial conceptual value).

We believe that the values we selected for the non- dimensional parameters in Stommel's and Munk's model fall within the relevant ranges of values of the dimensional parameters (see our detailed response to minor comment #6). We agree that our paper has two foci - one "conceptual" and the other "quantitative" (i.e. related to the world ocean).

Major comment:

The solution (3) to the Stommel model is indeed the most general, but this form rather obscures the essential physics in the physically-relevant limit of small α (i.e. the boundary current width is much smaller than the basin width). The authors erroneously state that in this limit, the solution becomes linear in x and can satisfy just one boundary condition. However, a more careful expansion of the exponential terms leads to a more complete solution.

I prefer to see this by assuming α is small and hence $\frac{\partial^2}{\partial x^2} \gg \frac{\partial^2}{\partial y^2}$. Thus (1) is well approximated by:

$$\alpha\frac{\partial^2\psi}{\partial x^2} + \frac{\partial\psi}{\partial x} \approx \sin(\pi y)$$

the solution to which is

$$\psi \approx (x - 1 + e^{-\alpha x})\sin(\pi y)$$

This solution consists of the Sverdrup (1947) solution in the basin interior – the first two terms in brackets on the right-hand side – and a Stommel (1948) western boundary current correction – the third tern in brackets on the right-hand side.

Mathematically, the dropping of the $\alpha\frac{\partial^2}{\partial x^2}$ term in (1) means that the particular integral is instead formed by balancing $\partial\psi/\partial x$ against the wind stress curl on the righthand side. However, the same result can be obtained through a careful treatment of the limit of small α in the two exponential terms in the more general solution.

The implications are that the western boundary current transport is:

- **approximately equal (and opposite) to the Sverdrup gyre transport**
- **independent of the linear drag coefficient, α;**
- **independent of the basin aspect ratio, δ.**

These conclusions are at odds with those stated in the manuscript. I do accept that in the case that α becomes larger, the boundary current transport, and indeed the entire nature of the solution changes, but it is hard to see what relevance this

has to a large-scale ocean basin.

Response: The assumption, $\frac{\partial^2}{\partial x^2} \gg \frac{\partial^2}{\partial y^2}$ that underlies the referee's comment, implies that the general solution of the associated homogeneous equation is y-independent i.e. the y-dependence of the solution is identical to that of the inhomogeneous forcing term. In our model, this assumption translates to $\frac{1}{\delta^2} = 0$ in the Laplacian $\nabla^2 = \delta^2 \frac{\partial^2}{\partial x^2} + \frac{\partial^2}{\partial y^2}$ [given by (2) in the manuscript]. While this y-independent limit can yield a fast-flowing WBC in Stommel's model, it completely undermines the role of basin's aspect ratio (δ) in determining the transport of the WBC, which is the main sermon of our paper (as is evident from the paper's title). For large scale circulation, typical values of $\delta < 0.5$ yield $\frac{1}{\delta^2} > 1$ i.e. setting $\frac{1}{\delta^2} = 0$ is inconsistent with the intended "quantitative" applications. The alternative is to employ the general solution of equation (1) without assuming y-independence of the Laplacian, which is precisely what we did in our paper.

Moreover, Bye and Veronis (1979) succinctly established the $\delta-$dependence of the Sverdrup transport. In terms of our scaling this correction can be derived by noting that since $\alpha = \epsilon/\delta^2$, equation (1) of the manuscript implies:

$$\left(\epsilon \frac{\partial^2}{\partial x^2} + \frac{\epsilon}{\delta^2} \frac{\partial^2}{\partial y^2}\right) \psi + \frac{\partial \psi}{\partial x} = \sin(\pi y)$$

where $\epsilon = (r/\beta L_x)$ is a proxy of damping and the non-dimensional width of the WBC. Under the assumption of small damping i.e. $\epsilon \ll 1$, the term $\frac{\epsilon}{\delta^2}\frac{\partial^2 \psi}{\partial y^2}$, cannot be neglected in the interior solution when $\delta^2 \sim O(\epsilon)$ i.e. the Sverdrup balance becomes a function of δ in this case. The latter two bullet points that the referee makes lead to the unacceptable result that the strength of the WBC (that is equal in magnitude to the δ-dependent Sverdrup transport) is not determined by either of the model parameters α (or ϵ) and δ!

To appreciate this subtle issue one should compare a square basin, where $\delta = 1$, with a "narrow and long channel-like" basin where $\delta \ll 1$. In a square basin, the classical approach of equating $\partial\psi/\partial x$ to $\sin(\pi y)$ works well since the North-South gradient of the zonal velocity (represented by $\partial^2\psi/\partial y^2$) is small and can be neglected from the interior solution. However, in a "channel-like" ocean this quantity is large and cannot be neglected from the balance of terms in the interior solution. Surely, an examination of the 3 vorticity terms in the interior ($\partial\psi/\partial x$, wind-stress and $\partial^2\psi/\partial y^2$) clarifies that the WBC in the "channel-like" ocean should be weaker compared to a square ocean. Clearly, in the referee's approach there is no difference between the two oceans.

Here, we take the opportunity to thank the referee for his comment. To reconcile our approach with the existing literature, we will re-write the paper with ϵ as the parameter for damping (instead of α). We will also include the aforementioned comparison between a square and "channel-like" basin to further emphasize the conceptual aspect of our study.

Changes: The entire paper was re-written with ϵ as the parameter for damping (instead of α). Lines 232 - 262 in the revised version of the manuscript underscore the 'physical' meaning of the vorticity terms in the interior of the basin in both models. This further adds to the conceptual aspect of this paper and presents our results in a more intuitive framework.

Minor comments:

1. I don't understand why the authors estimate the boundary current transport rather than simply calculate the maximum value of the streamfunction which gives the actual western boundary transports. If I follow correctly, the authors also invoke the Stommel scaling for the boundary layer width, but that only holds

in the low α limit

Response: The reviewer is right in that a simpler definition could have been used to estimate the transport. However, the definition based on the maximum point of the streamfunction gives a width of about 500 km in 10,000 km basin while our definition gives a width of about 100 km in the same basin. Moreover, using Stommel's scaling to obtain our ad-hoc definition of the boundary layer width [i.e. $\epsilon = r/(\beta L_x)$] makes the paper more accessible to oceanographers that are inclined towards observations or numerical modeling.

The expression for transport [given by (4) in the manuscript] is valid for the referee's definition of boundary layer width as well and the choice of the WBC's width does not alter the conclusions presented in our paper. We thank the referee for bringing this to our attention. In the revised manuscript, we will further emphasize that the results are not sensitive to the choice of WBC's width.

Changes: Lines 121 - 126 in the revised version of the manuscript discuss how our results are independent of the definition of the WBC's width.

2. It might be helpful to many readers to state the original equations, before nondimensionalising.

Response: We will accept an editorial decision on this matter but since both forms of the vorticity equation – dimensional and non-dimensional – appear in so many textbooks and research papers we thought that presenting both versions is redundant.

Changes: We accepted the editorial decision and included the original dimensional equation — see equation (1) (line 73) in the revised version of the manuscript.

3. γ is the non-dimensional magnitude of the wind stress curl, not the wind stress

Response: We thank the referee for pointing this out. We will correct this in the revised manuscript.

Changes: Appropriate corrections were made in lines 79 and 248 of the revised manuscript.

4. In figure 1(d), why is the eastern boundary condition not satisfied? Response: Figure 1(d), depicts the analytically obtained, non-dimensional streamfunction for Munk's model. In Munk's model the stream function, given by (7), is a function of $|\alpha| = \mu \frac{L_x}{\beta L_y^4}$ and does not vanish identically even for small $|\alpha|$ at either boundary (although the values of the streamfunction at the boundaries are rather small). For large values of $|\alpha|$, the value of the streamfunction at the boundary is no longer close to 0 (as it is for smaller $|\alpha|$) and we see the less than optimal behaviour as depicted in Figure 1(d).

We thank the referee for his input and will emphasize this further in the revised manuscript.

Changes: Lines 145-147 discuss the subtlety of why the analytic stream function for M50's model is not well behaved for large ϵ. We further underscore the crudeness of the analytic stream function in line 203.

5. I'm really struggling with the numerical and theoretical boundary current transport scalings in figure 3, especially the upper panel for the Stommel

gyre. I understand that the authors will state that these results support their conclusions, but they are at odds with the basic dynamics of the low α limit (see major comment above). The explanation in lines 194-189 of what has been done to obtain the theoretical scalings, and why, is confusing (to me at least).

Response: The results shown in Figure 3 highlight the consistency of our theoretical/analytic findings with (dimensional!) numerical simulations. Our response to the major comment above provides the explanation of the consistency between our dimensional numerical simulations and the non-dimensional analysis based on our scaling.

Changes: Figure 3 was re-drawn with ϵ as the abscissa and the results are consistent with our findings.

6. Regarding figure 4, are you seriously suggesting that $\alpha = 0.5$ is an appropriate value for the East Australian Current? This would imply the failure of geostrophy, for example.

Response: The parameter $\alpha = rL_x/(\beta L_y^2)$ for each WBC was estimated by substituting $\beta = 2 \times 10^{-11}$ m^{-1}s^{-1}, Rayleigh friction coefficient $r = 1/10$ (days)$^{-1}$ and the typical dimensions (L_x and L_y) of the basin. Other choices of the Rayleigh friction coefficient do not alter the results. Figure 1 below depicts the results for $r = 1/20$ (days)$^{-1}$ and the same values of β, L_x and L_y.

We thank the referee for suggesting this. If requested, we will be happy to include the attached figure in the revised manuscript.

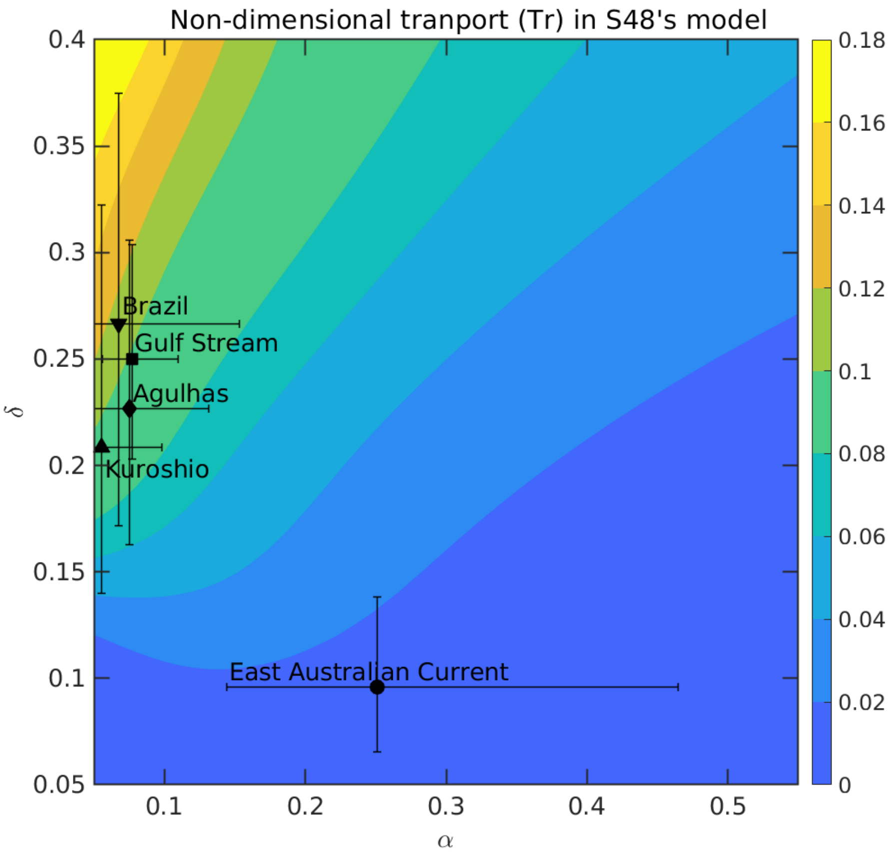

Figure 1: Alternative figure to panel (a) of Figure 4

Changes: The alternative figure above was not used because the manuscript was re-written with ϵ as the damping parameter. Figure 4 was re-drawn with ϵ as the abscissa and the new figure is presented in the revised manuscript.

7. Following on from point 6, there are numerous other processes that are likely in influence the width of real world western boundary currents ahead of linear bottom drag and lateral friction. These include relative vorticity (Fofonoff, 1954; Charney, 1955),stratification (the deformation radius emerges as a natural length scale), bottom topography (e.g., Hughes and de Cuevas, 2001), eddy fluxes (e.g., Eden and Olbers, 2010).

Response: We agree. However, none of these works addressed the role of basin's aspect ratio in determining the transport of the WBC.

Changes: No changes were made per this minor comment because addressing the issue highlighted by the referee in this comment is beyond the scope of this study.

References:
Bye, J. A. T., and George Veronis. "A correction to the Sverdrup transport." Journal of Physical Oceanography 9.3 (1979): 649-651.

On the role of domain aspect ratio in the westward intensification of wind-driven surface ocean circulation

Kaushal Gianchandani[1], Hezi Gildor[1], and Nathan Paldor[1]

[1]Fredy & Nadine Herrmann Institute of Earth Sciences, Hebrew University of Jerusalem, Edmond J. Safra Campus - Givat Ram, Jerusalem, 9190401, Israel

Correspondence: Nathan Paldor (nathan.paldor@mail.huji.ac.il)

Abstract. The two seminal studies on westward intensification, carried out by Stommel and Munk over 70 years ago, are revisited to elucidate the role of the domain aspect ratio (i.e. meridional to zonal extents of the basin) in determining the transport of the western boundary current (WBC). We examine the general mathematical properties of the two models by transforming them to differential problems that contain only two parameters — the domain aspect ratio and the non-dimensional damping (viscous) coefficient. Explicit analytical expressions are obtained from solutions of the non-dimensional vorticity equations and verified by long-time numerical simulations of the corresponding time-dependent equations. The analytical expressions as well as the simulations, imply that in Stommel's model both the domain aspect ratio and the damping parameter contribute ~~equally~~ to the non-dimensional transport of the WBC. However, the transport increases as a cubic power in the aspect ratio and decreases linearly with the damping coefficient. On the other hand, in Munk's model the WBC's transport ~~varies linear~~ increases linearly with the domain aspect ratio, while the damping ~~parameter~~ coefficient plays a minor role only. This finding is employed to explain the weak WBC in the South Pacific. The decrease in transport of the WBC for small domain aspect ratio results from the decrease in Sverdrup transport in the basin's interior because the meridional shear of the zonal velocity cannot be neglected as an additional vorticity term.

1 Introduction

As was noted by Henry Stommel, in the opening sentence of his seminal 1948 study "Perhaps the most striking ~~characteristic of the surface circulation in an ocean basin is the east-west asymmetry:~~ feature of the general oceanic wind-driven circulation is the intense crowding of streamlines near the western borders of the oceans." These strong and narrow ~~pole-ward directed currents~~poleward directed currents, often referred to as ~~the~~ "western boundary currents" (WBCs)~~flow along the western boundary of the ocean basins while the return equator-ward flow is~~ , counterbalance the weak and wide equatorward (Sverdrup) flow in the interior of the basin. In the North Atlantic this current is the Gulf Stream, and it was known to oceanographers and explorers for a few centuries — see Stommel (1958) for a historical review. Similar WBCs exist in other basins as well and these include the Kuroshio in the North Pacific and the Brazil current in the South Atlantic. These currents transport large amount of heat from low to high latitudes, thus playing an important role in the climate system. The winds overlying, though, are easterlies along the equator (the Trade winds) and westerlies around 40° N. There are no strong northward winds along the western boundaries of the ocean basins and, as is well understood now, the WBCs are not obviously correlated with the overlying wind patterns. Interestingly, two such WBCs lie in the Pacific viz. the Kuroshio and the East Australian current (EAC). Both the Kuroshio and the EAC are centered close to 26° latitude in their respective hemispheres and are driven by similar wind stresses and are adjacent to a $\sim$ 2000 km long coastline. Despite these structural similarities, the maximal volumetric transport of the Kuroshio current is 55 Sv (1 Sv = $10^6\ \mathrm{m^3 s^{-1}}$) (Qiu, 2019) whereas that of the EAC is around 30 Sv (Archer et al., 2017). The maximum velocity that EAC attains is also substantially smaller than that of the Kuroshio (Campisi-Pinto et al., 2020).

~~Henry~~ Stommel, apparently in his first oceanography paper (Stommel, 1948, hereafter referred to as S48) was the first to formulate a simple, yet comprehensive, mathematical model of the WBCs [see e.g. Kunzig (1999)]. S48 is now regarded as a seminal paper in theoretical physical oceanography (e.g. http://empslocal.ex.ac.uk/people/staff/gv219/classics.d/oceanic.html). S48's model probably provides the simplest explanation for the existence of WBCs: in this linear and frictional model on the $\beta-$plane the ocean is taken to be a flat bottom rectangle forced by a cos(latitude)-dependent zonal wind pattern. Walter Munk further extended this work to a different frictional (viscous) parameterization and a more general form of the wind stress (Munk, 1950, hereafter referred to as M50).

In the last 70 years, both models have been modified and extended to further explore the phenomenon of westward intensification in different settings or to evaluate the importance of different specific processes and terms in the governing equations (Munk and Carrier, 1950; Veronis, 1966a, b; Pedlosky, 2013; Vallis, 2017, and references therein).

As in S48 and M50, a large number of these subsequent studies employed the dimensional form of the governing equations which are the time-independent rotating linearized shallow water equations compounded by friction and forcing. These dimensional models include numerous parameters: the zonal and meridional extents of the basin; either the coefficient of linear drag (i.e. the coefficient in the Rayleigh frictional term) or the kinematic eddy viscosity (i.e. the coefficient in parameterization of the viscous term); the amplitude (and possibly meridional structure) of the wind stress; the gradient of Coriolis frequency ($\beta-$effect). On the other hand, a few studies (Welander, 1976; Bye and Veronis, 1979) employed the alternate, concise, approach of non-dimensionalising the governing equation (or the vorticity equation) to investigate the depth averaged wind-driven ocean circulation. The non-dimensional approach not only simplifies the problem by reducing the number of dimensional parameters in the model to fewer non-dimensional ones but also brings out some salient features associated with the problem which are difficult to unveil in the dimensional formulation.

By employing a non-dimensional approach, Welander (1976) successfully identified a zonally uniform regime in both S48's and M50's models of wind-driven ocean circulation and using the same approach, Bye and Veronis (1979) derived a correction to the Sverdrup transport in S48's model. The aforementioned studies highlighted the importance of the ratio between meridional and zonal extents of the basin as one of the two fundamental parameters in both S48's and M50's models. The aim of this study is to further elaborate on the role of the domain aspect ratio (defined here as the ratio between the basin's meridional and zonal extents) in S48's and M50's models of westward intensification. In particular, we examine the role of domain aspect ratio in the transport of the WBC as was first hypothesized by Bye and Veronis (1979) in the context of S48's model, "... the tendency of north-south diffusive processes to be more significant in basins with a large (***small** in the present scaling*) aspect ratio makes sense physically and may play a quantitative role in the transport of the western boundary current." We also examine the relevance of our results to the observed difference in strengths of the five WBCs in the world ocean.

The paper is organized as follows. Section 2 outlines our proposed scaling [which is slightly different from the one employed in Welander (1976); Bye and Veronis (1979)] that reduces the number of parameters in the vorticity equations corresponding to S48's and M50's models from five dimensional ones to two non-dimensional ones — one of which is the domain aspect ratio (the other is damping). The solution for the stream function in the two cases is outlined and using this we obtain the expression for the non-dimensional transport of the WBC in both S48's and M50's models. The applicability of the analytical expression of transport for relevant values of the model parameters is validated in Section 3 by simulating the time-dependent equations. We discuss the results and conclude in Section 4. We also note that there were some typos in the expressions of zonal velocity and sea surface height (but not the stream function itself) in S48 and for completeness, we list them in Appendix A. These typos do not change the scientific conclusions drawn in S48.

2 The two-parameter differential problems, their solutions and ~~transport~~ the transports of the WBC

2.1 S48's non-dimensional counterpart

~~We begin by scaling~~ S48's dimensional vorticity equation for the spatial structure of the stream function, ψ, is given by:

$$r\nabla^2\psi + \beta\frac{\partial\psi}{\partial x} = \tau_0\frac{\pi}{\rho_0 H_0 L_y}\sin\left(\frac{\pi y}{L_y}\right) \tag{1}$$

where r is the Rayleigh friction coefficient, β is the meridional gradient of Coriolis frequency and τ_0 is the amplitude of wind-stress. The operator ∇^2 is the two dimensional Laplacian, H_0 is the mean depth of the barotropic ocean with density ρ_0, L_y is the meridional dimension (and L_x is the zonal dimension) of the basin. The velocity components in the zonal and meridional directions, u and v, are related to the stream function via: $u = \frac{\partial\psi}{\partial y}$ and $v = -\frac{\partial\psi}{\partial x}$.

We begin by scaling (1) as follows: x (the zonal coordinate) on L_x~~(the basin's zonal extent)~~; y (the meridional coordinate) on L_y ~~(the basin's meridional extent)~~ and ψ ~~(the stream function)~~ on $\gamma\beta L_y^3$ where ~~$\gamma = \tau_0\left(\frac{\pi}{\rho_0 H_0 \beta L_y^2}\right)\left(\frac{L_x}{\beta L_y^2}\right)$~~ $\gamma = \tau_0\frac{\pi}{L_y}\left(\frac{L_x}{\rho_0 H_0 \beta^2 L_y^3}\right)$ is the non-dimensional amplitude of the wind stress ~~(and τ_0 is the wind's dimensional amplitude) with β — the meridional gradient of the Coriolis frequency, H_0 — the depth of the basin and ρ_0 — the water density of the~~

~~barotropic ocean~~curl. With this scaling the non-dimensional form of S48's vorticity equation is:

$$\alpha\frac{\epsilon}{\delta^2}\nabla^2\psi+\frac{\partial\psi}{\partial x}=\sin(\pi y) \tag{2}$$

where

$$\alpha\epsilon=r\left(\frac{L_x}{\beta L_y^2}\right)\frac{r}{\beta L_x},\quad \nabla^2=\delta^2\frac{\partial^2}{\partial x^2}+\frac{\partial^2}{\partial y^2}. \tag{3}$$

From this point onwards, both the variables and the operators in the differential equation(s) are non-dimensional while dimensional quantities will be accompanied by an asterisk (*). Here ∇^2 is the non-dimensional Laplacian, $\delta=\frac{L_y}{L_x}$ is the ratio of meridional and zonal extents of the basin (refereed to as the domain aspect ratio) and $\cancel{\alpha}$ ϵ is the non-dimensional ~~parameter (referred to as~~ width of the WBC (and also a proxy of the damping)~~proportional to $r\sim 1/10$ — the Rayleigh friction coefficient~~. The definition of the non-dimensional stream function implies that the zonal velocity and the meridional velocity are given by, $u=\frac{\partial\psi}{\partial y}$ and $v=-\delta\frac{\partial\psi}{\partial x}$, respectively. It is evident from (2) and (3) that the two parameters, $\cancel{\alpha}$ ϵ and δ, govern the structure of the flow in the basin. The no normal flow conditions at the basin's boundaries mandate that the stream function ψ satisfies the boundary conditions: $\psi(x,0)=\psi(1,y)=\psi(x,1)=\psi(0,y)=0$.

~~It should be stressed that due to the different scaling employed in the two works, our α in differs from the corresponding coefficient of damping in Bye and Veronis (1979). Moreover, we use~~ We note that the term domain aspect ratio ~~(δ) to refer to the ratio between meridional to zonal dimensions of the basin which is reciprocal~~ in the present study, $\delta=\frac{L_y}{L_x}$, is the inverse of the domain aspect ratio ~~defined by Bye and Veronis (1979)~~ used in Bye and Veronis (1979) who derived a non-dimensional equation similar to (2).

As has been stated earlier, the non-dimensional formulation lumps the five dimensional parameters in S48's model — zonal and meridional extent of the basin, gradient of Coriolis frequency, wind stress amplitude and Rayleigh friction coefficient — into just two non-dimensional ones: $\cancel{\alpha}$ ϵ and δ (~~that appears in the first term of~~ both of which appear only in the Laplacian operator). ~~The interplay between the three terms in the inhomogeneous partial differential vorticity equation, , can be easily interpreted by repeating the procedure employed in~~ Following S48~~to obtain the general form of solutions of . An~~, an explicit expression for the solution for ψ in (2) is given by:

$$\psi(x,y)=\frac{1}{\alpha\pi^2}\frac{\delta^2}{\epsilon\pi^2}\sin(\pi y)(pe^{Ax}+qe^{Bx}-1) \tag{4}$$

where

$$p=\frac{1-e^B}{e^A-e^B}$$

$$q=1-p$$

and

$$A = -\cancel{\frac{1}{2\alpha\delta^2}}\frac{1}{2\epsilon} + \frac{\pi}{\delta}\cancel{\sqrt{1+\frac{1}{4\pi^2\alpha^2\delta^2}}}\sqrt{1+\frac{\delta^2}{4\pi^2\epsilon^2}},$$

$$B = -\cancel{\frac{1}{2\alpha\delta^2}}\frac{1}{2\epsilon} - \frac{\pi}{\delta}\cancel{\sqrt{1+\frac{1}{4\pi^2\alpha^2\delta^2}}}\sqrt{1+\frac{\delta^2}{4\pi^2\epsilon^2}}.$$

As is evident from (4), the spatial structure of the stream function is controlled by both ~~α~~ ϵ and δ. ~~Fig. 1~~Panels (a) ~~,~~and (c) of Fig. 1 depict the stream ~~function for two α~~functions for two ϵ-regimes of S48's model: (i) weak damping [~~$\alpha \leq O(1)$~~$\epsilon \lesssim \delta^2$] and (ii) strong damping [~~$\alpha > O(1)$~~$\epsilon \gtrsim \delta^2$]. For ~~$\alpha \leq O(1)$~~$\epsilon \lesssim \delta^2$, the solution ψ given by (4) becomes linear in x and thus can satisfy only one boundary condition out of two. This solution is commonly assumed to approximate the exact solution for ψ in the frictionless interior of the basin while a different approximation applies in the narrow, frictional, boundary layer adjacent to $x = 0$. Fig. 1(a) depicts this narrow boundary layer for ~~$\alpha = 0.1$~~ $\epsilon = 0.1\delta^2$ where the stream function first decreases fast with x at small x and then increases slowly with x for large x. ~~In the range of $\alpha \geq O(1)$~~For $\epsilon \gtrsim \delta^2$, the solution, ψ, is symmetric about $x = \frac{1}{2}$ and can satisfy the two boundary conditions, $\psi(0, y) = 0 = \psi(1, y)$. This is demonstrated in the symmetric stream function depicted in Fig. 1(c) for ~~$\alpha = 10$~~$\epsilon = 10\delta^2$. The explicit expressions of ψ in the two ranges of ~~α~~ ϵ are given in the Appendix B.

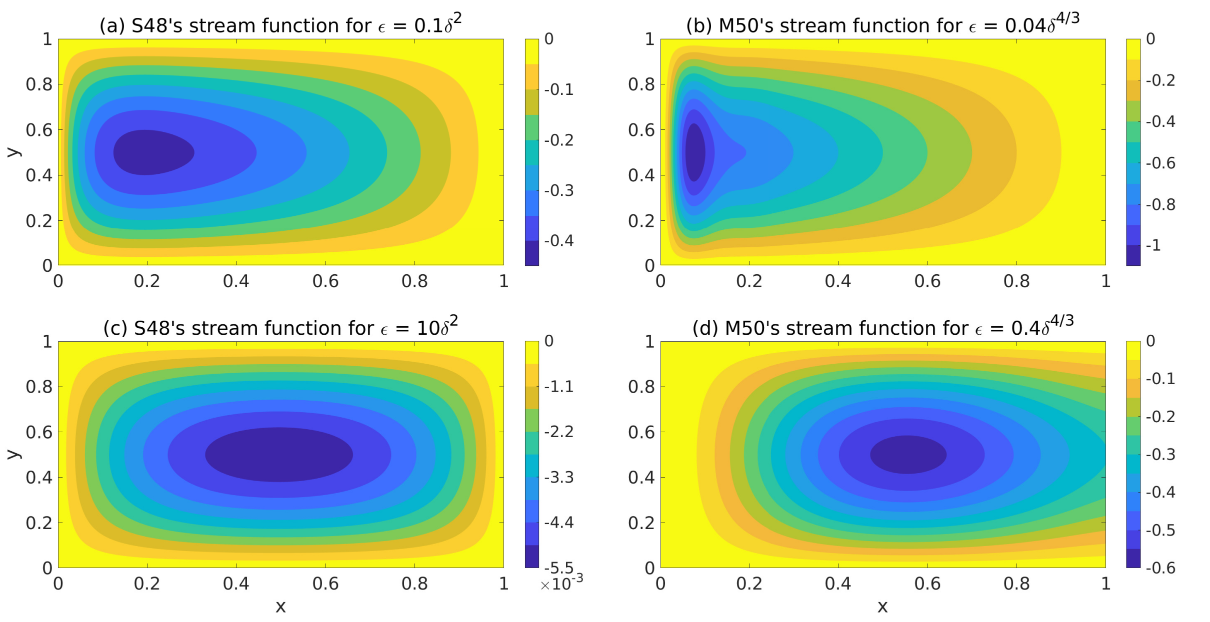

Figure 1. The stream functions in different ϵ regimes of ~~the α parameter-space in the two~~ S48's and M50's models for $\delta = 2\pi/10$: (a) ~~,~~and (b) weak damping [~~$\alpha \leq O(1)$~~ $\epsilon \lesssim \delta^2$ in S48's model and ~~$|\alpha| \leq O(10^{-3})$~~ $\epsilon \lesssim 0.1\delta^{4/3}$ in M50's model] — there exists a narrow fast flowing current along the western edge of the basin~~;~~. (c) ~~,~~and (d) strong damping [~~$\alpha > O(1)$~~ $\epsilon \gtrsim \delta^2$ in S48's model and ~~$|\alpha| > O(10^{-3})$~~ $\epsilon \gtrsim 0.1\delta^{4/3}$ in M50's model] — the stream function is (nearly) symmetric about $x = 0.5$ which indicates that there is no westward intensification.

In ~~the non-dimensional~~ S48's model, ~~the width of the WBC is given by $\epsilon = \alpha\delta^2$ which can be derived from the balance between the Rayleigh friction term and the advection of planetary vorticity in the WBC i.e. $\frac{r}{\beta L_x}$. The definition of the steam function implies that the zonal velocity and the meridional velocity are given by, $u = \frac{\partial \psi}{\partial y}$ and $v = -\delta\frac{\partial \psi}{\partial x}$, respectively. We define the (non-dimensional)~~ we define the transport of the WBC as the product of its width~~and the mean meridional velocity~~, ϵ, and the average of the meridional velocity, $v = -\delta\frac{\partial \psi}{\partial x}$, between the western edge of the basin, $x = 0$, and $x = \epsilon$ evaluated along $y = \frac{1}{2}$ i.e. $Tr = \epsilon\left(\frac{1}{\epsilon}\int_0^\epsilon -\delta \left.\frac{\partial \psi}{\partial x}\right|_{y=\frac{1}{2}} dx\right)$. ~~Though the definition of the WBC's width is somewhat arbitrary for definitiveness we chose it to be ϵ.~~ The integral in the ~~the~~ definition of the transport, Tr, simplifies to the product of the domain aspect ratio and the difference in the values of the stream function evaluated at $x = 0$ and $x = \epsilon$ along $y = \frac{1}{2}$, i.e. $Tr = \delta\left[\psi\left(0, \frac{1}{2}\right) - \psi\left(\epsilon, \frac{1}{2}\right)\right]$. Substituting the boundary condition $\psi\left(0, \frac{1}{2}\right) = 0$ and using the explicit solution (4) yields:

$$Tr = \frac{\delta^3}{\epsilon\pi^2}(1 - pe^{A\epsilon} - qe^{B\epsilon}). \tag{5}$$

This expression will be compared below to its counterpart in M50's model and will be compared in section 3 with transports calculated by numerical simulations.

Here, we note that the definition of the WBC's width is somewhat arbitrary and for definiteness we choose it to be ϵ [as in Welander (1976); Bye and Veronis (1979); Vallis (2017)]. However, the conclusions drawn in this study are independent of the precise definition; for instance, the width of the WBC can also be defined as the value of x at which the stream function reaches an extremum. According to this definition the WBC's width, ϵ' equals $\sim 5\epsilon$ and the corresponding transport is given by $Tr' = \frac{\delta^3}{5\epsilon\pi^2}(1 - pe^{5A\epsilon} - qe^{5B\epsilon})$. Both, expressions of Tr and Tr', yield that the transport of the WBC in S48's model varies as $\sim \frac{\delta^3}{\epsilon}$.

2.2 M50's non-dimensional counterpart

The non-dimensional counterpart of M50's vorticity equation, obtained by employing the scaling proposed in this study in a similar manner to that of S48 [refer to Munk (1950) for the dimensional equation], is given by:

$$\cancel{\alpha} - \frac{\epsilon^3}{\delta^4}\nabla^4\psi + \frac{\partial \psi}{\partial x} = \sin(\pi y) \tag{6}$$

where

$$\cancel{\alpha}\epsilon = \cancel{-\mu\frac{L_x}{\beta L_y^4}}\frac{1}{L_x}\left(\frac{\mu}{\beta}\right)^{1/3}, \quad \nabla^4 = \delta^4\frac{\partial^4}{\partial x^4} + 2\delta^2\frac{\partial^4}{\partial x^2 \partial y^2} + \frac{\partial^4}{\partial y^4} \tag{7}$$

where ~~μ ($\sim 10^4$)~~ μ is the (dimensional) horizontal eddy viscosity coefficient. We note that contrary to ~~, α in~~ (3), the sign in front of the first term in (7) is negative. This dissimilarity arises because, unlike the parametrization in S48, in M50's model the damping is parametrized by ~~a biharmonic function~~the two dimensional bilaplacian operator. Also, in addition to stream function vanishing at the edges of the basin another set of boundary condition has to be specified to solve the 4^{th} order equation (6). The additional boundary conditions employed by M50 originate from the inclusion of lateral viscosity which implies that there should be no tangential flow at the basin's edges i.e. $\left.\frac{\partial\psi}{\partial x}\right|_{x=0,1} = \left.\frac{\partial\psi}{\partial y}\right|_{y=0,1} = 0$. Following the mathematical steps in M50 yields the following approximate solution of (6):

$$\psi = -\sin(\pi y)\left[1 - x + \cancel{\frac{1}{\lambda}}\epsilon e^{\cancel{\lambda(x-1)}(x-1)/\epsilon} - e^{\cancel{-\lambda(x/2)}-(x/2\epsilon)}\xi(\cancel{\lambda}\epsilon)\right] \qquad (8)$$

~~where $\lambda = \left(\frac{1}{-\alpha\delta^4}\right)^{1/3}$~~, and $\xi(\cancel{\lambda}\epsilon) = \left[\cos\left(\cancel{\frac{\sqrt{3}\lambda x}{2}}\frac{\sqrt{3}x}{2\epsilon}\right) + \cancel{\frac{1-2/\lambda}{\sqrt{3}}}\frac{1-2\epsilon}{\sqrt{3}}\sin\left(\cancel{\frac{\sqrt{3}\lambda x}{2}}\frac{\sqrt{3}x}{2\epsilon}\right)\right]$.

~~Fig. 1~~Panels (b) ~~,~~and (d) ~~depicts~~ of Fig. 1 depict the stream function for small and large damping in M50's model. For large damping the stream function shown in Fig. 1(d) is not entirely symmetric about $x = \frac{1}{2}$. Also, unlike the behavior of the stream function in S48's model, the stream function in M50's model skews more towards the eastern boundary with the increase in damping. This, less than optimal, behavior of the stream function in M50's model occurs because the stream function does not vanish identically along the eastern boundary and is, instead, a function of ~~α~~ ϵ itself (although, ~~this value is not large~~for small ϵ, the zonal velocity there is small compared to the rest of the basin).

We turn now to the estimation of the WBC's transport in M50's model. As was done in S48's model, this transport is also defined as the product of the boundary layer width (ϵ~~given by $(-\alpha\delta^4)^{(1/3)} \equiv (|\alpha|\delta^4)^{(1/3)}$ in M50's model~~) and the mean meridional velocity of the current between $x = 0$ and $x = \epsilon$ along $y = \frac{1}{2}$. Following the arguments laid out in the previous section [see the paragraph above (5)] an expression for transport can be obtained by multiplying the domain aspect ratio by the difference of the stream function values between $x = 0$ and $x = \epsilon$ along $y = \frac{1}{2}$. Furthermore, substituting the boundary condition $\psi\left(0, \frac{1}{2}\right) = 0$ yields $Tr = -\delta\psi\left(\epsilon, \frac{1}{2}\right)$. Evaluating ψ in (8) at $\left(\epsilon, \frac{1}{2}\right)$ ~~where~~ for $\epsilon \ll 1$ yields the following simplified expression for the WBC's transport in M50's model:

$$Tr = \delta\left(1 - e^{(-1/2)}\left[\cos\left(\frac{\sqrt{3}}{2}\right) + \frac{1-2\epsilon}{\sqrt{3}}\sin\left(\frac{\sqrt{3}}{2}\right)\right]\right). \qquad (9)$$

~~In S48's model~~ As anticipated by, the transport of the WBC ~~,~~ in S48's model [given by (5)~~,~~] is governed by both damping (~~α~~ϵ) and domain aspect ratio (δ). ~~This is in agreement with the findings of Bye and Veronis (1979).~~ However, in M50's model the dependence of the WBC's transport on the two parameters is strikingly different~~. At least to zeroth order, the WBC's transport in M50's model is independent of α and is governed solely~~ : the transport is governed primarily by δ and is weakly dependent on ϵ. In the next section we validate ~~this claim using~~ these claims using (dimensional) numerical simulations and then apply our results to the present-day world ocean.

3 Numerical simulations and application to the world ocean

The numerical simulations described below were carried out using the time-dependent, forced-dissipative, rotating shallow water equation (SWE) dimensional solver that was successfully used in previous studies. The solver employs the finite difference method to solve SWEs on the $\beta-$plane and the simulations are carried out on an Arakawa C grid with leapfrog time difference scheme. Though the solver can include nonlinear terms, these terms were neglected in the present application. The reader should refer to Gildor et al. (2016) and Shamir et al. (2019) for a more detailed description of the solver. ~~The reader should also note that dimensional variables mentioned in this section are accompanied by an asterisk (∗).~~

The simulations presented here were carried out in a barotropic ocean with the same characteristics as in S48 i.e. on an equatorial $\beta-$plane ($f_0 = 0$), forced by a wind stress that varies as $-\tau_0 \cos\left(\dfrac{\pi y^*}{L_y}\right)$. Three of the dimensional parameters remained fixed in all the simulations presented below — the gradient of Coriolis frequency (given by $\beta = 2\times10^{-11}\ \mathrm{m^{-1}s^{-1}}$), the zonal extent of the basin (L_x = $10000\ \mathrm{km}$) and the amplitude of the prescribed forcing ($\tau_0 = 0.2\ \mathrm{Nm^{-2}}$). The other two dimensional parameters in the two WBC models i.e. the damping coefficients [Rayleigh friction coefficient (r) in S48's model and horizontal eddy viscosity (μ) in M50's model] and the meridional extent of the basin (L_y) are varied to examine the effect of ~~α~~ ϵ and δ on the transport. We note that keeping τ_0 fixed and varying L_y will yield different values of γ in the simulation, however, since we scale our ψ^* on $\gamma\beta L_y^3$ and only look at the non-dimensional transport we do not have to account for the effects of changes in γ. The results are consistent with what one would obtain by keeping only β and L_x fixed and varying τ_0 along with the damping coefficients and L_y to keep γ constant. The boundary conditions are: the (dimensional) zonal and meridional velocities vanish along the basin's meridional and zonal boundaries respectively, i.e. $u^*|_{y^*=0,L_y} = v^*|_{x^*=0,L_x} = 0$. The numerical solver is integrated until a steady state is reached. The steady state of the time-dependent simulations is defined as the state at which the dependent variables in the SWEs [dimensional zonal velocity (u^*), meridional velocity (v^*) and sea surface height (η^*)] cease to evolve for sufficiently long time.

~~Fig. 2~~Panels (a) ~~,~~and (c) ~~depicts~~ in Fig. 2 depict the numerically obtained, non-dimensional stream function $\left(\psi = \dfrac{\psi^*}{\gamma\beta L_y^3}\right)$ in the steady state for the dimensional parameters as in S48's model (and the corresponding values of ~~α~~ ϵ and δ are noted above these panels) while ~~Fig.2~~panels (b) ~~,~~and (d) ~~depicts~~ in Fig.2 depict the numerically obtained, non-dimensional ψ in the steady state for the parameters relevant to M50's model (and here too the corresponding values of ~~α~~ ϵ and δ are noted above these panels). The reader should note that the meridional extent (L_y) of the basin ~~in Fig. 2~~shown in panels (a) ~~,~~and (b) of Fig. 2 is $2\pi \times 1000$ km, whereas~~in Fig. 2~~, the meridional extent of the basin shown in panels (c) ~~,~~and (d) ~~, $L_y = \pi/2\times1000$~~ in Fig. 2 is $L_y = \pi/4 \times 1000$ km. In all four cases the shape of the stream function is very similar to the steady non-dimensional stream functions shown in Fig. 1 [panels (a) ~~,~~and (b)]. We note that for the given values of (~~α~~ϵ, δ), the ψs obtained from dividing the numerically calculated ψ^*s by the corresponding values of $\gamma\beta L_y^3$ ~~agree very well~~ are in agreement with the ψ calculated analytically for the same values of (~~α~~ϵ, δ) using (4) for S48's model and (8) for M50's model.

Fig. 2 depicts that in both S48's and M50's models, for a fixed value of ~~α~~ $\epsilon = 0.01$ (damping and the width of the WBC), the gradient of the stream function increases with δ~~while the~~. The higher zonal gradient of the stream function ~~(and, in turn, the~~ near the western boundary yields a larger meridional velocity, thus increasing the transport of the WBC (given by the product of width and average meridional velocity of the WBC)~~decreases with it. This indicates that~~. Clearly, δ exercises a control over the transport of the WBC and hence cannot be ignored.

Fig. 3 compares the analytic and numerically computed values of the non-dimensional transport (Tr) of the WBC in S48's and M50's models as a function of ~~$|\alpha|$~~ ϵ for several values of δ. The solid lines denote the analytic value of Tr obtained

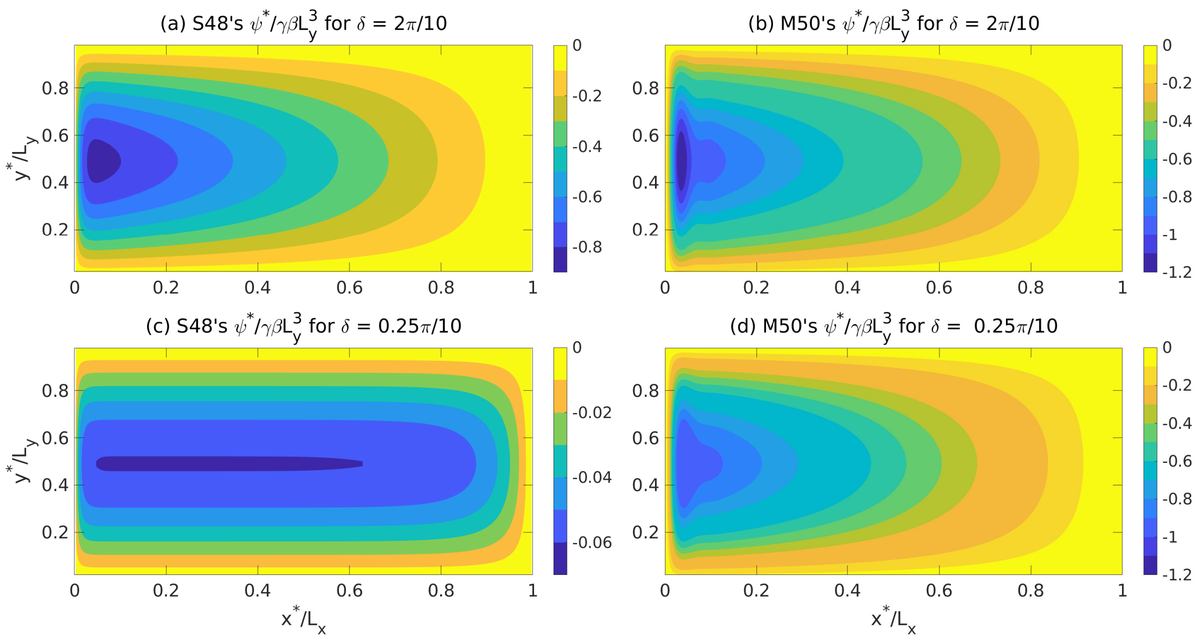

Figure 2. Numerically obtained, ~~non-dimensionalized,~~ non-dimensional stream functions for $\epsilon = 0.01$ and $L_x = 10,000$ km. (a) ~~for~~ S48's model ~~— $(\alpha, \delta) = (0.1, 2\pi/10)$ and~~ with $\delta = 2\pi/10$, (b) ~~for~~ M50's model ~~— $(\alpha, \delta) = (-2\times 10^{-5}, 2\pi/10)$; panels~~ with $\delta = 2\pi/10$. Panels (c) ~~,~~and (d) are the same as (a) ~~,~~and (b) but for ~~$\delta = 0.5\pi/10$~~$\delta = 0.25\pi/10$ i.e.~~Note that ψ^*, x^* and y^* are scaled on $\gamma\beta L_y^3$, L_x and L_y respectively~~. ~~Also,~~ the meridional extent of the basin ~~(L_y)~~ is one-eighth of that in (a) and (b)~~was chosen to be one-fourth of that~~. Note the different colorbars in panels (a) and (c).

from the expressions given by (5) and (9). The 'numerical transport' of the WBC is obtained by taking the product of δ and $-\dfrac{\psi^*(\epsilon, \frac{1}{2})}{\gamma\beta L_y^3}$. Here, $\psi^*\left(\epsilon, \dfrac{1}{2}\right)$ is the value of the steady state dimensional stream function at $\left(\epsilon, \dfrac{1}{2}\right)$ obtained from the results of the numerical simulation for a given set of parameters which correspond to a certain ~~(α, δ); $\epsilon = \alpha\delta^2$ in S48's and $\epsilon = (|\alpha|\delta^4)^{1/3}$ in M50's model~~(ϵ, δ).

As is evident by Fig. 3(a), the analytic and numerically calculated non-dimensional transports of the WBC ~~are in agreement for large values of α in S48's model. However, for small values of both α and δ the numerically calculated transport of the WBC is smaller than the analytic one. This is because,~~ in S48's model ~~, the gradient of the stream function given by is very large near the western edge of the basin i.e. the stream lines are 'squished' together, which is not the case in numerical simulations carried out under the same setting. Fig. ??~~are in good agreement. Fig. 3(b) shows that the analytic ~~transport~~ transports of the WBC ~~is~~ in M50's model are nearly independent of ~~$|\alpha|$ and is~~ ϵ and are governed primarily by δ. The numerically calculated ~~transport~~ transports of the WBC ~~shows a similar behavior, however, there is a notable dependence of the transport on $|\alpha|$ for small values of the parameter~~depicted by the dashed lines in Fig. 3(b) show a similar dependence on δ but in contrast to the approximate analytic expression these transports vary slightly with ϵ. We also note that there is a discernible difference ~~in~~ between the analytically estimated and numerically calculated values of transport in M50's model for nearly all values of (~~$|\alpha|$~~ϵ,

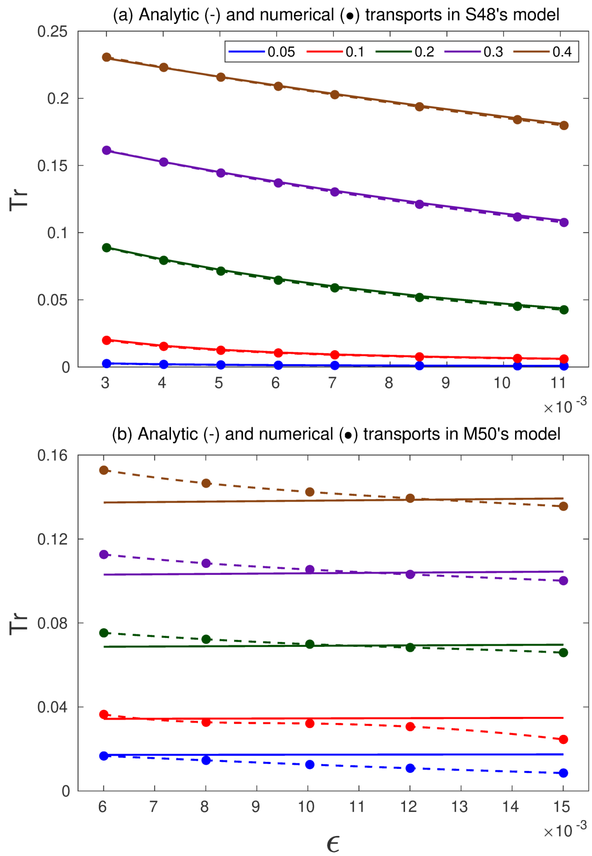

Figure 3. Comparison between analytically (solid lines) and numerically (dots) calculated values of transport (Tr) as a function of ~~$|\alpha|$~~ ϵ for different values of δ in (a) S48's and (b) M50's models. The dashed lines depict the cubic spline interpolated curves between the numerically calculated transports (dots).

δ). This is because the ~~value of~~ expression for the stream function ~~obtained under the assumption $\epsilon \ll 1$ does not hold for large values of $|\alpha|$ and the contribution from the neglected terms becomes significant~~for M50's model, [i.e. (8)] only crudely approximates the actual stream function.

Fig. ~~??~~ 4 depicts the non-dimensional transport of the WBC in S48's [panel (a)] and M50's models [panel (b)] as contours on (~~α, δ~~ϵ, δ) plane. The contours were obtained by interpolating (using the cubic spline method) between the numerically calculated values of the WBC's transport as shown in Fig. ~~??~~3. As is evident from Fig. ~~??~~4(a), the non-dimensional transport is a function of both ~~α~~ ϵ and δ in S48's model. On the other hand, Fig. ~~??~~4(b) shows that the transport of the WBC is ~~nearly independent of $|\alpha|$~~ only weakly dependent on ϵ and is governed primarily by δ (~~contours nearly parallel~~ the contours are nearly parallel to the abscissa). The position of the different WBCs in the ~~(α, δ) parameter space ($|\alpha|, \delta$) for M50's model~~(ϵ, δ) parameter space is marked with different symbols and the errorbars account for the inaccuracies in the assigned values of the

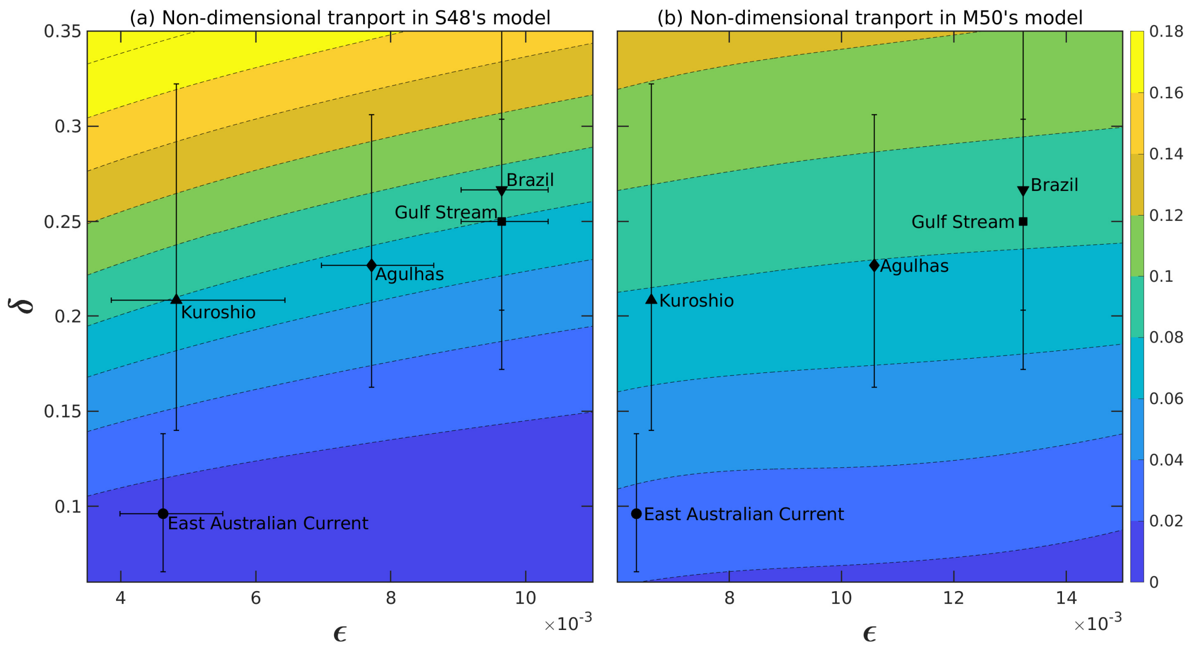

Figure 4. The non-dimensional transport of the western boundary current (WBC) as a function of ~~α~~ ϵ and δ in (a) S48's model and (b) M50's model. The different WBCs in the world ocean are depicted with different symbols and the ~~errorbars~~ error bars denote the possible variability of parameters that can occur because of an error in estimating the zonal and meridional extents of the basins that contain the WBC. The error in ~~$|\alpha|$~~ ϵ is not accounted for in (b) because the WBC's transport in M50's model is (nearly) independent of ~~$|\alpha|$~~ϵ. The East Australian Current's (EAC) non-dimensional transport, as calculated from both S48's and M50's models, is less than the other four WBCs. The uncertainty in ~~α~~ δ for the ~~EAC~~ Brazil Current extends up to ~~0.9~~ 0.375 in ~~S48's model~~both the models, the contours have been restricted to better resolve the ~~other four~~ boundary currents. The range between which the non-dimensional transport varies is similar in both the models.

zonal and meridional extents of the basins. The details of how the irregular basins in the world ocean are approximated with rectangles are discussed in Appendix C. The error in ~~$|\alpha|$~~ ϵ has been omitted from ~~??~~4(b) because the WBC's transport in M50's model is nearly independent of ~~$|\alpha|$~~ϵ. Despite the large uncertainty in the damping parameters (relevant in S48's model only) and domain aspect ratios (relevant in both S48's and M50's models) of the five WBCs, the non-dimensional transport of the East Australian Current (EAC) is distinctly smaller than that of the other WBCs.

4 Summary and Discussions

Since the introduction of the S48's and M50's models about 70 years ago, numerous theoretical and numerical investigations have been carried out to further explore the characteristics of westward intensification (Munk and Carrier, 1950; Stommel, 1958; Hogg and Johns, 1995; Pedlosky, 2013; Vallis, 2017, and references therein). Both S48's and M50's dimensional models clearly bring out the contribution of each source of vorticity: damping, planetary gradient and wind forcing in producing the characteristic east-west asymmetry of the flow in a basin. However, it is difficult to quantify the contribution of each of the five dimensional parameters (L_x, L_y, β, τ_0 and r/μ) to the transport of WBC, using the dimensional models. A better alternative is to combine several dimensional parameters to yield a system with fewer non-dimensional parameters as was employed by, for example, Welander (1976) to identify a zonally uniform regime in ocean circulation and by Bye and Veronis (1979) to identify the correction to the Sverdrup transport in context of S48's original model.

In this article, we address the issue raised by Bye and Veronis (1979) regarding the effect of domain aspect ratio on the WBC's transport by providing explicit expressions of the non-dimensional transport in both S48's and M50's models. These expressions are then benchmarked against numerical simulations of the time dependent, forced-dissipative, rotating shallow water equations. Both the analytic expressions and steady state simulations show that the WBCs' transports depend on both ~~α~~ ϵ and δ in S48's model~~and both the parameters have a similar effect on the transport $\left(Tr\sim\frac{\delta}{\alpha}\right)$~~, however, a change in δ has a stronger effect on Tr when compared to a change in ϵ $\left(Tr\sim\frac{\delta^3}{\epsilon}\right)$. In contrast, the transport of the WBC in M50's model is nearly independent of ~~α~~ ϵ and is governed primarily by δ $(Tr\sim\delta)$.

In the traditional description of the S48 model the flow is decomposed into two parts: A slow, anti-cyclonic flow in the inner-basin where the velocities are tiny so frictional effects can be neglected and a return boundary flow where the frictional vorticity associated with the zonal shear of the poleward directed velocity, balances the planetary vorticity advected by this velocity. According to this paradigm the WBC simply returns the frictionless equatorward Sverdrup transport of the inner-basin so its transport is independent of the friction coefficient and since the (dissipation) Laplacian term does not affect the Sverdrup interior flow, the transport of the WBC should also be independent of the domain aspect ratio. The present study demonstrates that the assumption of small damping, $\epsilon \ll 1$, implies that only the term $\epsilon\frac{\partial^2\psi}{\partial x^2}$ of the Laplacian in (2) can be neglected in this limit while the second term, $\frac{\epsilon}{\delta^2}\frac{\partial^2\psi}{\partial y^2}$, cannot be neglected in the interior solution when $\delta^2 \sim O(\epsilon)$. The implication of our analysis is that the Sverdrup interior flow depends on δ for sufficiently small δ and therefore so does the (return) transport of the WBC.

To appreciate this subtle issue one should compare a square basin, where $\delta = 1$, with a narrow and long "channel-like" basin where $\delta \ll 1$. In a square basin, the classical approach of equating $\frac{\partial\psi}{\partial x}$ to $\sin(\pi y)$ in the inner basin works well since the North-South gradient of the zonal velocity (represented by $\frac{\partial^2\psi}{\partial y^2}$) is small and can be neglected from the interior solution. However, in a "channel-like" ocean this quantity is large and cannot be neglected from the balance of terms in the interior solution. An examination of the three vorticity terms in the interior [$\frac{\partial\psi}{\partial x}$, $\frac{\partial^2\psi}{\partial y^2}$ and $-\sin(\pi y)$] clarifies that the transport of the WBC (as well as the equatorward transport in the interior) in a "channel-like" ocean should be smaller compared to a square ocean since the meridional shear of the zonal velocity lowers the vorticity induced by the curl of the wind stress. In an extreme "channel-like" ocean with $\frac{\epsilon}{\delta^2} \gg 1$ the only term that can balance $\frac{\partial^2\psi}{\partial y^2}$ is $\frac{\partial\psi}{\partial x}$ that implies a strong, equatorward directed velocity. Indeed, as was shown by Welander (1976) for a small domain aspect ratio, a boundary layer develops along the basin's eastern boundary in which the strong current flows equatorward.

In M50's model the vorticity balance of the interior is more involved since the bilaplacian dissipation operator (∇^4) has 3 terms, each of which with a coefficient of different power of δ. Thus, the distinction between terms associated with the inner basin and those with the boundary solution is not as clear as in S48's model. However, under the assumption of small damping, $\epsilon \ll 1$, the third term in the ∇^4 operator [given by (7)] cannot be neglected for $\delta^4 \sim O(\epsilon^3)$. Similar to S48's model, the vorticity balance in the interior, which is determined in this limit by the interplay of 3 terms $\frac{\partial^4 \psi}{\partial y^4}$, $\frac{\partial \psi}{\partial x}$ and $-\sin(\pi y)$, yields a $\delta-$dependent equatorward transport. This $\delta-$dependent transport in the interior is balanced by an equal, poleward-directed, transport along the western boundary. Although the vorticity associated with $\frac{\partial^4 \psi}{\partial y^4}$ is not as intuitive as that associated with $\frac{\partial^2 \psi}{\partial y^2}$ in S48's model the change it entails in Sverdrup's interior solution is similar.

The results derived here highlight an important effect that was overlooked in the classical/traditional WBC theory, namely, the effect of the domain aspect ratio on the Sverdrup solution of the inner basin which results from the meridional shear of the zonal velocity in a narrow zonal channel.

The non-dimensional formulation presented here does not alter the physical basis of the ~~two~~ S48 and M50 models. We emphasize that the dimensional transport (calculated from the product of the non-dimensional transport and $\gamma \beta L_y^3 H_0$) in S48's model varies linearly with the Rayleigh friction coefficient (r) while in M50's model it is nearly independent of the eddy viscosity (μ). ~~On the other hand, in~~ In both models the transport ~~varies linearly with the wind-forcing amplitude (τ_0)~~is linear with magnitude of the wind-stress curl.

The application of our results to present-day ocean attributes the small transport of the EAC compared to the other WBCs to the geometry of the South Pacific ocean. ~~However~~In reality, factors other than the domain aspect ratio may also be important in determining the transport. For instance, the Brazil current's volumetric transport is low (especially in the northern part) because the current is largely confined to the continental shelf (Stramma et al., 1990). Temperature-driven buoyancy fluxes can also affect the transport of a WBC (Hogg and Gayen, 2020).

It is highly plausible that with a different arrangement of the continents in previous geologic times, the small domain aspect ratio that persisted in the ocean at that time could not support a strong WBC. Thus, the resulting higher pole to equator temperature gradient might have strongly affected the Meridional Overturning Circulation. This hypothesis should be addressed in a future work.

Acknowledgements. The authors thank D. Marshall and another anonymous reviewer whose comments were helpful in distilling some of the subtle points addressed in this work.

Financial support. This research was supported by the ISF-NSFC joint research program (grant number 2547/17).

Code availability. The numerical model used in this work can be downloaded from https://github.com/kaushalgianchandani/SWEsolver

Data availability. No data were used or generated in this theoretical research.

Author contributions. All authors contributed equally to this work.

Competing interests. The authors declare no conflict of interest.

Appendix A: Typos in Stommel (1948)

There are some typos in the expression for u [equation (21)] and η [equation (23)] in Stommel (1948). The correct expressions are given as:

$$
\begin{aligned}
u &= \gamma(b/\pi)\cos(\pi y/b)\left(pe^{Ax}+qe^{Bx}-1\right) && \text{(A1)}\\
\eta &= -(F/gD)\cos(\pi y/b)(e^{Ax}p/A+e^{Bx}q/B)\\
&\quad -(f\gamma/g)(b/\pi)^2\sin(\pi y/b)(pe^{Ax}+qBe^{Bx}-1)\\
&\quad +(\partial f/\partial y)(\gamma/g)(b/\pi)^3\cos(\pi y/b). && \text{(A2)}
\end{aligned}
$$

For the reader's perusal, the variables in the aforementioned equations are the same as the ones defined in Stommel (1948). Fig. A1 provides excerpts from Stommel (1948) over which, the corrections have been highlighted.

Appendix B: Limiting cases of stream function ψ in S48's model

In the limit $\cancel{\alpha < O(1)}\epsilon \leq \delta^2$, the solution ψ tends to:

$$\lim_{\cancel{\alpha<O(1)}\epsilon\leq\delta^2}\psi(x,y) = \cancel{\frac{c_1}{\alpha\pi^2}}c_1\frac{\delta^2}{\epsilon\pi^2}\sin(\pi y)(x) \qquad \text{(B1)}$$

where $\cancel{c_1 = \lim_{\alpha<O(1)} A}\, c_1 = \lim_{\epsilon\leq\delta^2} A$ is a number $\ll 1$. On the other hand, in the limit of $\cancel{\alpha > O(1)}\epsilon > \delta^2$, the solution ψ becomes:

$$\lim_{\cancel{\alpha>O(1)}\epsilon>\delta^2}\psi(x,y) = \cancel{\frac{1}{\alpha\pi^2}}\frac{\delta^2}{\epsilon\pi^2}\sin(\pi y)[p(e^{c_2x}+e^{c_2(1-x)})-1] \qquad \text{(B2)}$$

where $\cancel{c_2 = \lim_{\alpha>O(1)} A = \frac{\pi}{\delta}}\, c_2 = \lim_{\epsilon>\delta^2} A = \frac{\pi}{\delta}$ and $p = \dfrac{e^{c_2}-1}{e^{2c_2}-1}$. The function $\cancel{\lim_{\alpha>O(1)}\psi(x,y)}\,\lim_{\epsilon>\delta^2}\psi(x,y)$ is symmetric about $x = \dfrac{1}{2}$.

The velocity components u and v may be obtained from (8) by simple differentiation of the stream function

$$u = \gamma(b/\pi)^{\cancel{2}} \cos(\pi y/b)(pe^{Ax} + qe^{Bx} - 1) \quad \ldots\ldots\ldots\ldots\ldots\ldots \quad (21)$$

$$v = -\gamma(b/\pi)^2 \sin(\pi y/b)(pAe^{Ax} + qBe^{Bx}) \quad \ldots\ldots\ldots\ldots\ldots\ldots \quad (22)$$

cos(πy/b)

The value of h at any point referred to the value of h at the origin may now be obtained by integration of (1) and (2).

$$h(x,y) = -(F/gD)(e^{Ax}p/A + e^{Bx}q/B) - \cancel{(b/\pi)^2(F/gD)(pAe^{Ax} + qBe^{Bx})[(\cos \pi y/b) - 1]}$$

$$- \left\{(f\gamma/g)(b/\pi)^2 \sin(\pi y/b) \cancel{-(\partial f/\partial y)(\gamma/g)(b/\pi)^3[\cos(\pi y/b) - 1]}\right\}\left\{pe^{Ax} + qe^{Bx} - 1\right\} \quad . (23)$$

$+ (\partial f/\partial y)(\gamma/g)(b/\pi)^3 \cos(\pi y/b)$

Figure A1. Corrections to u and h indicated over excerpts from Stommel (1948).

Appendix C: Zonal and meridional extents of the five western boundary currents in present-day world ocean

To determine the zonal and meridional extents of a basin containing a WBC, we identified the mean initiation and termination latitudes of each WBC based on the available literature. The Gulf Stream begins at the tip of Florida ($\sim$25° N) and runs upto $\sim$38° N where it breaks of into hot and cold rings (Hogg and Johns, 1995). The Kuroshio originates from the bifurcation of North Equatorial current at 12 - 13° N, although this bifurcation point can vary between 10 - 15° N (Qiu and Lukas, 1996); it separates from the Japan coast at 35° N as a meandering current colloquially known as the Kuroshio extension which stretches as far as $\sim$ 38° N (Kida et al., 2016). The East ~~Madagascar-Agulhus~~ Madagascar-Agulhas current, in the South Indian ocean, runs from 20° S to 40° S (Lutjeharms et al., 1981; Gordon, 1985; Lutjeharms, 2006) — however the current retroflects between 38° S to 40° S (Quartly and Srokosz, 1993). Moreover, the African continental landmass ends close to 35° S. The Brazil current begins between 10° S and 12° S (Peterson and Stramma, 1991; Stramma et al., 1990) but the intense current attains its intense speed characteristic of a WBC only when it crosses the Vitoria-Trindade Ridge at 20.5° S (Evans et al., 1983). This current separates from the coastline at a mean value of 36° S $\pm$ 1.1° (Olson et al., 1988). The last of the five WBCs in the world ocean is the East Australian Current (EAC) that extends from 18° S to around 35° S (Boland and Church, 1981; Ridgway and Godfrey, 1994) but a characteristic southward flow is evident only when EAC crosses 22° S (Ridgway and Dunn, 2003); the current usually separates from the coast at 33° S (Archer et al., 2017).

We define the meridional extent (L_y) is defined as the distance between the initiation and termination latitudes of the WBC. On the other hand, to determine the zonal extent (L_x) we calculated the distances between the land masses at both the initiation latitude and termination latitude. The average of the two distances is defined as the typical L_x for any given WBC.

Table C1. Dimensions of the gyres that contain the five western boundary currents in the present-day world ocean.

Current	Western edge of the basin		Eastern edge of the basin		Basin's dimensions	
	Initiation	Termination	Initiation	Termination	Zonal (L_x)	Meridional (L_y)
Gulf Stream	25° N 80° W	38° N 75° W	25° N 16° W	38° N 10° W	6000 ± 400 km	1500 ± 200 km
Kuroshio	13° N 125° E	35° N 140° E	13° N 92° W	35° N 121° W	12000 ± 3000 km	2500 ± 400 km
Madagascar-Agulhas	20° S 50° E	35° S 20° E	20° S 116° E	35° S 116° E	7500 ± 800 km	1700 ± 350 km
Brazil	21° S 40° W	35° S 54° W	21° S 13° E	35° S 19° E	6000 ± 400 km	1600 ± 500 km
East Australian	22° S 150° E	33° S 152° E	22° S 70° W	33° S 72° W	12500 ± 2000 km	1200 ± 250 km

For instance, the approximate initiation and termination coordinates for the Kuroshio are 13° N, 125° E and 35° N, 140 E respectively, which yields $L_y \approx 2500\ \mathrm{km}$. The distances to the opposite landmass, the North American continent (which forms the eastern boundary of the basin) as calculated from the initiation coordinate and termination coordinate are $\sim 9000\ \mathrm{km}$ and $\sim 15000\ \mathrm{km}$ respectively. Thus, the typical zonal extent of the basin is assumed to be $12000\ \mathrm{km}$.

The mean dimensions L_x and L_y for all the five WBCs in the world ocean are given by Table 1. The 'error' in L_y accounts for the variation between different references of the initiation and termination latitudes and the error in L_x is the deviation of the measured zonal distances along initiation and termination latitude from the mean value. Based on these values of L_x and L_y a range of parameters damping (α) and domain aspect ratio (δ) corresponding to every WBC was estimated and these values of α and δ were employed it to distinguish between the five WBCs. Typical values of L_x and L_y for the ocean basins that contain the WBCs were also estimated using the mean streamlines in the ocean as calculated by Maximenko et al. (2009) — these values were well within the range cited in Table C1.

References

Archer, M. R., Roughan, M., Keating, S. R., and Schaeffer, A.: On the Variability of the East Australian Current: Jet Structure, Meandering, and Influence on Shelf Circulation, Journal of Geophysical Research: Oceans, 122, 8464–8481, 2017.

Boland, F. and Church, J.: The East Australian current 1978, Deep Sea Research Part A. Oceanographic Research Papers, 28, 937–957, 1981.

Bye, J. and Veronis, G.: A Correction to the Sverdrup Transport, Journal of Physical Oceanography, 9, 649–651, 1979.

Campisi-Pinto, S., Gianchandani, K., and Ashkenazy, Y.: Statistical tests for the distribution of surface wind and current speeds across the globe, Renewable Energy, 149, 861 – 876, 2020.

Evans, D. L., Signorini, S. R., and Miranda, L. B.: A Note on the Transport of the Brazil Current, Journal of Physical Oceanography, 13, 1732–1738, 1983.

Gildor, H., Paldor, N., and Ben-Shushan, S.: Numerical simulation of harmonic, and trapped, Rossby waves in a channel on the midlatitude β-plane, Quarterly Journal of the Royal Meteorological Society, 142, 2292–2299, 2016.

Gordon, A. L.: Indian-Atlantic Transfer of Thermocline Water at the Agulhas Retroflection, Science, 227, 1030–1033, 1985.

Hogg, A. M. C. and Gayen, B.: Ocean Gyres Driven by Surface Buoyancy Forcing, Geophysical Research Letters, p. e2020GL088539, 2020.

Hogg, N. G. and Johns, W. E.: Western boundary currents, Reviews of Geophysics, 33, 1311–1334, 1995.

Kida, S., Mitsudera, H., Aoki, S., Guo, X., Ito, S.-i., Kobashi, F., Komori, N., Kubokawa, A., Miyama, T., Morie, R., et al.: Oceanic fronts and jets around Japan: a review, in: “Hot Spots” in the Climate System, pp. 1–30, Springer, 2016.

Kunzig, R.: The Restless Sea: Exploring the World Beneath the Waves, WW Norton & Company, 1999.

Lutjeharms, J., Bang, N., and Duncan, C.: Characteristics of the currents east and south of Madagascar, Deep Sea Research Part A. Oceanographic Research Papers, 28, 879–899, 1981.

Lutjeharms, J. R.: The Agulhas Current, vol. 5, Springer, 2006.

Maximenko, N., Niiler, P., Centurioni, L., Rio, M.-H., Melnichenko, O., Chambers, D., Zlotnicki, V., and Galperin, B.: Mean Dynamic Topography of the Ocean Derived from Satellite and Drifting Buoy Data Using Three Different Techniques*, Journal of Atmospheric and Oceanic Technology, 26, 1910–1919, 2009.

Munk, W. H.: On the wind-driven ocean circulation, Journal of Meteorology, 7, 80–93, 1950.

Munk, W. H. and Carrier, G. F.: The Wind-driven Circulation in Ocean Basins of Various Shapes, Tellus, 2, 158–167, 1950.

Olson, D. B., Podesta, G. P., Evans, R. H., and Brown, O. B.: Temporal variations in the separation of Brazil and Malvinas Currents, Deep Sea Research Part A. Oceanographic Research Papers, 35, 1971–1990, 1988.

Pedlosky, J.: Geophysical Fluid Dynamics, Springer Science & Business Media, 2013.

Peterson, R. G. and Stramma, L.: Upper-level circulation in the South Atlantic Ocean, Progress in Oceanography, 26, 1–73, 1991.

Qiu, B.: Kuroshio and Oyashio Currents☆, in: Encyclopedia of Ocean Sciences (Third Edition), edited by Cochran, J. K., Bokuniewicz, H. J., and Yager, P. L., pp. 384 – 394, Academic Press, Oxford, third edition edn., 2019.

Qiu, B. and Lukas, R.: Seasonal and interannual variability of the North Equatorial Current, the Mindanao Current, and the Kuroshio along the Pacific western boundary, Journal of Geophysical Research: Oceans, 101, 12 315–12 330, 1996.

Quartly, G. and Srokosz, M.: Seasonal Variations in the Region of the Agulhas Retroflection: Studies with Geosat and FRAM, Journal of Physical Oceanography, 23, 2107–2124, 1993.

Ridgway, K. and Dunn, J.: Mesoscale structure of the mean East Australian Current System and its relationship with topography, Progress in Oceanography, 56, 189–222, 2003.

Ridgway, K. and Godfrey, J.: Mass and heat budgets in the East Australian current: A direct approach, Journal of Geophysical Research: Oceans, 99, 3231–3248, 1994.

Shamir, O., Yacoby, I., Ziskin Ziv, S., and Paldor, N.: The Matsuno baroclinic wave test case, Geoscientific Model Development, 12, 2019.

Stommel, H.: The westward intensification of wind-driven ocean currents, Eos, Transactions American Geophysical Union, 29, 202–206, 1948.

Stommel, H.: The Gulf Stream: A Physical and Dynamical Description, Univ of California Press, 1958.

Stramma, L., Ikeda, Y., and Peterson, R. G.: Geostrophic transport in the Brazil Current region north of 20° S, Deep Sea Research Part A. Oceanographic Research Papers, 37, 1875–1886, 1990.

Vallis, G. K.: Atmospheric and Oceanic Fluid Dynamics: Fundamentals and Large-scale Circulation, Cambridge University Press, 2017.

Veronis, G.: Wind-driven ocean circulation—Part 1. Linear theory and perturbation analysis, in: Deep Sea Research and Oceanographic Abstracts, vol. 13, pp. 17–29, Elsevier, 1966a.

Veronis, G.: Wind-driven ocean circulation—Part 2. Numerical solutions of the non-linear problem, in: Deep Sea Research and Oceanographic Abstracts, vol. 13, pp. 31–55, Elsevier, 1966b.

Welander, P.: A Zonally Uniform Regime in the Oceanic Circulation, Journal of Physical Oceanography, 6, 121–124, 1976.